Framework modification of microporous silicates via gas-phase treatment with $ZrCl_4$

Gopalakrishnan G. Juttu and Raul F. Lobo *

Department of Chemical Engineering, University of Delaware, Newark, DE 19716, USA
E-mail: lobo@che.udel.edu

Received 11 May 1999; accepted 5 August 1999

The boron forms of the zeolite Beta (B-Beta) and SSZ-33 (B-SSZ-33) are treated with vapors of $ZrCl_4$ in an attempt to substitute the framework boron for zirconium. The resulting materials Zr-Beta and Zr-SSZ-33 are characterized by X-ray diffraction (XRD), solid state NMR, FTIR, pyridine adsorption and Raman spectroscopies. In the case of zeolite Beta, Zr substitutes the B present in the framework nearly in a one-to-one basis. No evidence is found in support of the tetrahedral Zr fully incorporated into the zeolite framework; Zr is only partially grafted to the zeolite framework giving rise to silanol groups adjacent to the Zr atom. No evidence of extra-framework zirconia is observed. For SSZ-33, the amount of zirconium incorporated is significantly less than the amount of boron present in the parent zeolite. Due to the size of $ZrCl_4$, a multidimensional 12-ring pore system is required for our procedure of Zr incorporation to be effective. Zr-Beta is an acid catalyst superior in activity to B-Beta for the isomerization of 1-butene.

Keywords: zeolite, vapor-phase treatment, boron Beta, zirconium, acid catalysis

1. Introduction

Incorporation of transition metals Ti, V, Fe, etc., into the zeolite framework has expanded the application of zeolites to catalytic processes other than acid catalysis [1–4]. For example, titanium silicalite, TS-1 [5,6], is commercially used in the partial oxidation of phenol. The amount of transition metal incorporated into the framework of microporous silicates is usually low (<5% by weight). In contrast, amorphous mixed oxides can have a significantly higher amount of transition metal component. The molecular dispersion of the transition metal is of critical importance for maximum activity and various syntheses have aimed at maximizing the dispersion of the transition metal component. The microporous nature of these transition metal containing zeolites provide the added advantage of improved selectivities and the potential to tailor-make shape-selective catalysts.

Amorphous transition metal oxide/silicate mixed oxides have been prepared by sol–gel synthesis [7,8,11–13] and other methods. The sol–gel synthesis of mixed oxides with atomically dispersed metal atoms –M–$(O–Si)_n$– is often difficult to achieve. Due to the differences in the reactivities of the precursor materials, the mixed oxides tend to segregate into phases of MO_x and SiO_2 [14]. The controlled hydrolysis to make atomically dispersed amorphous mixed oxides is possible but is often difficult to achieve in practice. For example, expensive precursor molecules that have pre-formed –M–O–Si– linkages [15,16] may be necessary. Terry et al. synthesized zirconium tris(*tert*-butoxy) siloxy complexes which are "single-source precursors" to amorphous zirconia–silica materials [15]. The pyrolysis of these materials gives rise to mixed oxides which have a large number of –M–O–Si– heterolinkages. Thermolysis of this precursor at 200 °C gives a material that has a surface area of 118 m^2/g and a BET pore volume of 0.84 cm^3/g. It is important to note that the "molecular precursors" have Zr in a 4+ oxidation state in a pseudo-tetrahedral coordination environment with oxygen and silicon in its first and second coordination spheres, respectively. This is very similar to the kind of coordination that could be formed in a zeolite framework. Though the thermolysis of these "single source" precursors can give a homogeneous distribution of Si and Zr in the oxide matrix, pyrolysis at temperatures >1000 °C leads to the formation of tetragonal and monoclinic phases of zirconia.

A criterion that has been used to predict if an atom can be in the tetrahedral coordination environment in a zeolite framework is the Pauling criterion, which suggests that for tetrahedral incorporation, $0.414 < \rho < 0.225$, where $\rho = r_c/r_a$ (r_c and r_a are the Shannon cation and anion radii, respectively [9]). But various materials have been synthesized that violate this criterion. For example, CIT-6 [10] has been synthesized with Zn in the framework that has $\rho = 0.548$. Since Zr has a $\rho = 0.541$, it is not unreasonable to expect that it is possible to incorporate Zr into the zeolite framework.

Miller [11] has shown that Zr–O–Si heterolinkage gives rise to acid sites in ZrO_2/SiO_2 mixed oxides and based on the model proposed by Tanabe [17], the acid sites can be either Brønsted or Lewis depending on the relative number of Zr and Si present. The mixed oxides are active for the

* To whom correspondence should be addressed.

isomerization of 1-butene whereas the pure oxides are both inactive.

Microporous silicates with transition metals in their framework have been synthesized by two routes:

- Direct synthesis: In this route, the transition metal is added to the zeolite synthesis gel, and it is incorporated directly during the crystallization of the zeolite [2,5,6].
- Post-synthetic treatment: After the zeolite is synthesized, it is treated by wet impregnation methods or vapor-phase treatments (especially borosilicates) [18,19].

Microporous titanium silicates with various structures (such as MFI (ZSM-5), MEL (ZSM-11), BEA (Beta), CON (SSZ-33)) have been synthesized by direct methods [20,21] and post-synthetic methods [19]. The characterization of these materials has been carried out extensively [22,23]; it is now widely accepted that the Ti is isolated in the framework, in a 4+ oxidation state and in a tetrahedral coordination environment. The presence of extra-framework Ti (as anatase) is detrimental for TS-1. The synthesis of zirconium-containing silicates has also been claimed in the MFI topology [24–26], but the coordination of Zr in these materials has not yet been proved conclusively. Only the direct synthesis method has been reported for Zr silicates.

Here we describe the synthesis and characterization of Zr zeolite Beta and zeolite SSZ-33 by the reaction of the corresponding borosilicate analogs with $ZrCl_4$ vapors. We choose the post-synthetic route over the direct synthesis method to:

- Prevent the formation of insoluble particles of $ZrOCl_2$ and ZrO_2 which are very easily formed upon contact of the Zr precursors with water. Hydrolysis of $ZrCl_4$ can lead to clusters of ZrO_2, decrease the number of molecularly dispersed Zr and promote detrimental secondary reactions.
- Since borosilicate analogs of Al-containing zeolites are easily prepared, this route offers the possibility of synthesis of a variety of Al-free materials.

The presence of Al in the Ti silicates is often detrimental to its catalytic application. The presence of Al leads to the Brønsted acid sites in TS-1, makes it hydrophilic leading to reduced activity, secondary reactions and lower selectivities [27,28] in the epoxidation of alkenes using hydrogen peroxide.

Large pore borosilicate zeolites Beta and SSZ-33 were chosen as starting materials. Since the boron can be easily removed from the framework [29], this composition facilitates the incorporation of Zr. Large pore zeolites are chosen because $ZrCl_4$ cannot enter the 10 MR pores (see below) of the zeolite. The Zr incorporation via gas phase probably occurs by a mechanism similar to that proposed for Ti [19], as shown in figure 1. This requires that the B^{3+} charge be balanced by a proton and, as a consequence, boron should be in a trigonal coordination environment (in dehydrated samples). As shown by Fild et al. [30], framework boron is trigonal if its charge is balanced by H^+ whereas when the charge on the boron is balanced by Na^+, the coordination

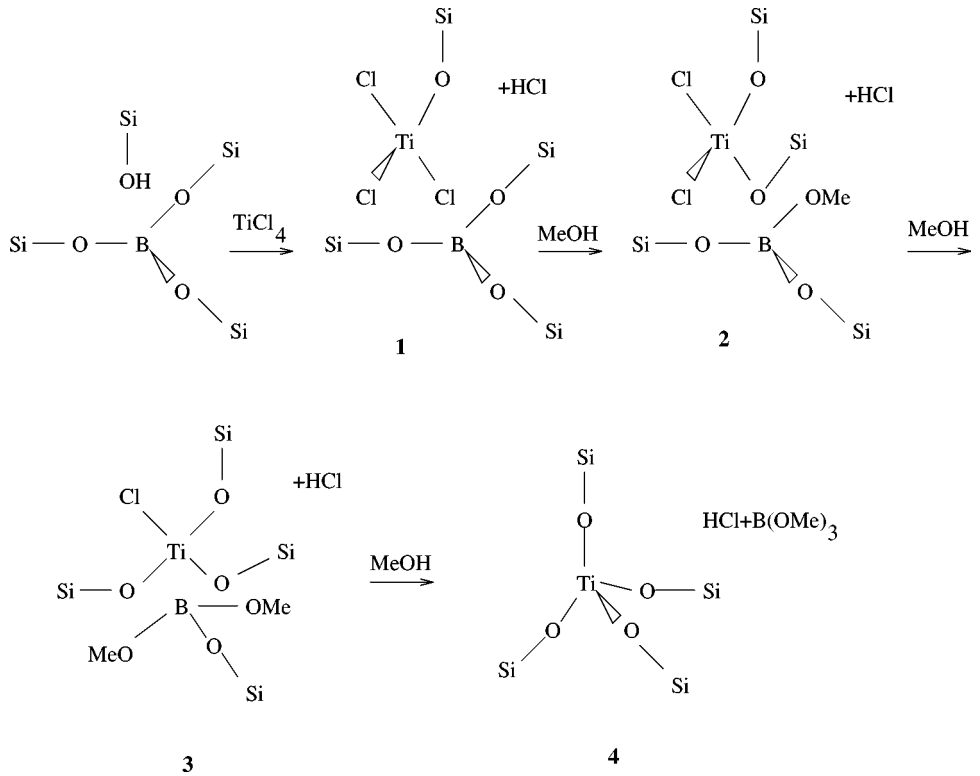

Figure 1. Mechanism for incorporation of Ti by gas-phase treatment (based on [19]).

is tetrahedral. All the borosilicates used in this work are converted to their acid form before the $ZrCl_4$ treatment.

We have found that in the case of Beta, the Zr replaces the framework B almost on a one-to-one basis. The Zr is only partially grafted to the framework and is not fully incorporated in a tetrahedral coordination. There is no evidence for the presence of extra-framework zirconia (based on Raman spectroscopy). Attempts to incorporate Zr into SSZ-33 did not result in the replacement of all the B by Zr. A multidimensional large pore zeolite is necessary for the complete incorporation of Zr by gas-phase treatment. Zr-Beta has superior catalytic activity over B-Beta for 1-butene isomerization.

2. Experimental

2.1. Zeolite synthesis

Zeolite boron Beta is synthesized following a method reported by Zones et al. [31]. The structure directing agent (SDA) used in the synthesis is 1,4-di(1′,4′-diazabicyclo[2.2.2]octane) butane hydroxide (figure 2). The SDA is synthesized from 1,4-diazabicyclo[2.2.2]octane (DABCO, 98% Aldrich) and 1,4-dibromobutane (99% Aldrich). 50 g of DABCO are dissolved in 400 ml of acetone (99.5% ACS grade, Aldrich). To this solution, 17.1 g of 1,4-dibromobutane in 100 ml acetone are added dropwise with continuous stirring. After 48 h (with vigorous agitation at room temperature), the product precipitates as a white powder and it is filtered and washed with tetrahydrofuran and ethyl ether. After elimination of the solvent under vacuum at room temperature, the product is exchanged into its hydroxide form using an ion-exchange resin (IONAC NA-38, OH^- form, J.T. Baker; five times in excess of the stoichiometric amount). The completion of the ion exchange is confirmed by titrating the solution with 0.1 N HCl. An ion exchange in excess of 97% is obtained.

The zeolite is synthesized from a gel of the following composition: $SiO_2 : 0.28R(OH)_2 : 0.017Na_2B_4O_7{\cdot}10H_2O : 60H_2O$, where R is the structure directing agent. Ludox AS-40 (40 wt% colloidal silica, Aldrich) is used as the source of silica. For example, 0.53 g of $Na_2B_4O_7{\cdot}10H_2O$ are completely dissolved in 40 ml of 0.28 M aqueous solution of the SDA. 6 g of Ludox AS-40 are added dropwise to this solution and the product is stirred for 30 min. The synthesis gel is then charged into PTFE lined stainless-steel autoclaves (Parr) and placed in an oven at 160 °C for 7 days. The autoclaves are rotated at 30 rpm during the synthesis.

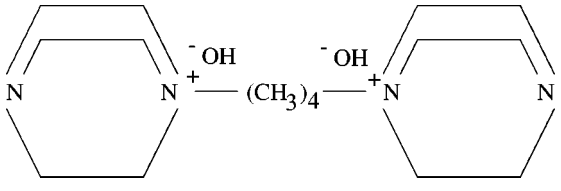

Figure 2. Structure directing agent (SDA) used in the synthesis of boron Beta.

The synthesis product is filtered and washed with deionized water. The as-made zeolite is calcined at 550 °C for 4 h in air (ramp rate of 2 °C/min). The calcined product is then converted to the ammonium form by three ion exchanges with 1.0 M solution of CH_3COONH_4 (1 g zeolite per 100 ml CH_3COONH_4 solution). Before further treatment, the zeolite was heated at 550 °C (heating rate 1 °C/min) to convert it to the acid form.

The as-made B-SSZ-33 samples were provided by S.I. Zones (Chevron). These samples are calcined at 550 °C (ramp rate 2 °C/min) for 4 h. They are converted to the proton form by three ion exchanges with 1.0 M solution of CH_3COONH_4 followed by calcination at 550 °C.

2.2. $ZrCl_4$ treatment

Zr is incorporated in the B-zeolites by contacting $ZrCl_4$ vapors with the zeolites. A schematic of the setup is shown in figure 3. The reactor is made of a silica-glass tube 2.5 cm in diameter with a coarse quartz frit in the center. The temperature of the reactor is controlled using a Lindberg Blue-M oven equipped with a Eurotherm 91E controller. Initially, 0.4 g of the zeolite are heated to 300 °C in a stream of dry argon gas for 3 h (flow rate 40 ml/min). The argon stream is then switched to pass over $ZrCl_4$ (0.4 g held at 250 °C; vapor pressure of $ZrCl_4 \approx 10$ Torr) before passing through the zeolite. About 0.2 g of $ZrCl_4$ is vaporized during the treatment procedure. After 4 h of this treatment, the argon is bubbled through warm methanol (50 °C). The argon with the methanol vapors is passed over the zeolite (by-passing the $ZrCl_4$) for 8 h with the zeolite held at 300 °C. The zeolite is then heated to 500 °C for 4 h in the stream of dry argon. The treated zeolite is finally washed

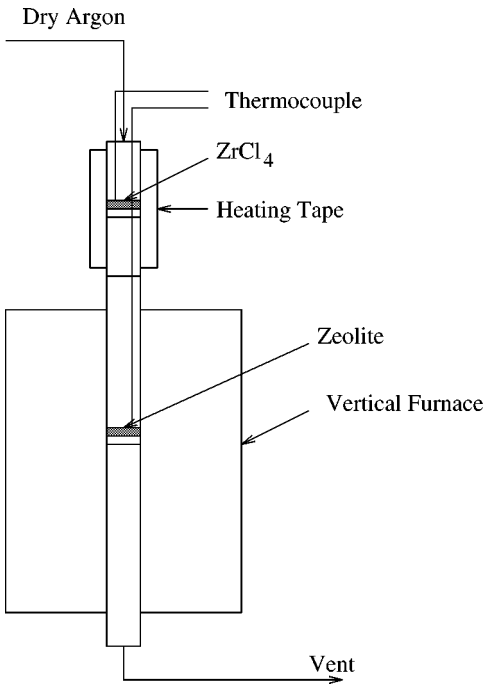

Figure 3. Diagram of the experimental setup.

with 100 ml methanol and 100 ml deionized water. The resulting materials will be denoted as Zr-Beta and Zr-SSZ-33.

2.3. Analytical

The X-ray powder diffraction (XRD) patterns were collected on a Phillips X'PERT diffractometer using Cu Kα radiation ($\lambda = 1.54186$ Å) and a gas-filled proportional detector. The diffraction profiles were scanned using the step mode over the range of $3^\circ < 2\theta < 50^\circ$ in steps of 0.02° 2θ with a step time of 15 s at each point. Fourier-transform infrared (FTIR) spectroscopy of the calcined samples was carried out on a Nicolet 510 FTIR spectrometer using the KBr pellet technique. For the FTIR spectrum of adsorbed pyridine, the sample was pressed on a tungsten mesh and placed in a specially designed IR cell. The IR cell has a circular chamber which can be evacuated to 10^{-1} Pa and heated to 200 °C. The windows of the cell are made of KBr. The sample was pressed onto a tungsten mesh and was placed in the path of the beam. Pyridine was introduced on the sample by flowing a stream of He saturated with pyridine. Pure dry He was subsequently flowed over the zeolite.

^{29}Si and ^{11}B solid state NMR were measured on a Bruker MSL-300 spectrometer at 59.63 and 96.31 MHz, respectively. ^{29}Si NMR spectra were obtained in a 7 mm zirconia rotor at a spin rate of 3 kHz with a $\pi/3$ pulse of 5 μs and a recycle delay of 30 s with ^{1}H-highpower decoupling. The CP-MAS ^{29}Si NMR were collected with a 2 ms contact time. The Raman spectra were collected on a Nicolet System 800 spectrometer fitted with a Raman accessory. The N_2 adsorption isotherms were obtained on a Micromeritics ASAP 2010 at 77 K. Elemental analyses were performed at the Galbraith Laboratories Inc., Knoxville, TN. The temperature-programmed desorption (TPD) and thermal gravimetric analysis (TGA) of isopropylamine were carried out simultaneously using a Cahn 2000 microbalance mounted within a high-vacuum chamber. A turbomolecular vacuum pump was used to evacuate the system to a pressure of 10^{-8} Pa. The desorbing species were analyzed using a Spectramass quadrupole mass spectrometer. Further details are provided in [48].

2.4. Catalysis

The isomerization of 1-butene is used as a test reaction to study the catalytic activity of the zeolite samples [49]. The reactor used is an in-house built silica-glass tube 25 cm long, 6 mm inside diameter with a 2 cm section in the middle flared to 13 mm diameter. A porous frit in the middle is used to support the catalyst. The reactor wall has an indentation in the middle to insert a thermocouple. The reactants and the products are analyzed using a GM Series 750P gas chromatogram with a flame ionization detector (FID). The products are separated using a 23% SP-1700 on 80/100 Chromosorb P AW filled in a stainless-steel tube column of length 30 ft and 1/8 inch outer diameter (Supelco). 0.16 g of the zeolite are loaded into the reactor and pretreated at 300 °C in a flow of 50 ml/min of dry He for 2 h. The feed has a composition of 20% butene and 80% helium. The total flow rate of the reactants is 100 ml/min. The reaction temperature is maintained at 150 °C.

3. Results and discussion

Figure 4 shows the X-ray diffraction patterns of B-Beta and Zr-Beta. As can be clearly observed, both samples are highly crystalline zeolite Beta and no loss of crystallinity is observed during the treatment procedure. The amount of Zr incorporated into the zeolite was approximately 0.053 g Zr/g zeolite (0.58 mmol Zr/g zeolite). The N_2 adsorption isotherms reveal that the microporosity of the sample is not significantly reduced by the treatment.

The results from the elemental analysis are summarized in table 1. Clear evidence for the reaction of $ZrCl_4$ with the B-Beta can be seen from the data. In contrast, the Zr content of Zr-SSZ-33 is much lower than that of Zr-Beta. For B-Beta, the mole ratio of $B/(B + Si) = 0.0625$ and that of Zr-Beta of $Zr/(Zr + B) = 0.045$. This shows that approximately, each atom of B is reacting with one atom (but not more) of Zr. The amount of Zr in the samples did not increase if the samples are contacted with $ZrCl_4$ vapors for a longer period of time. For B-SSZ-33, the mole ratios are $B/(B + Si) = 0.055$ and for Zr-SSZ-33 are $Zr/(Si + Zr) = 0.0224$. Not all the B is being replaced by Zr in the case of Zr-SSZ-33. At least 25% of the boron remains unreacted. Since the nature of the Zr present in these materials is not revealed by elemental analysis, other techniques must be used to distinguish the Zr present inside the crystal and that present outside the zeolite crystals.

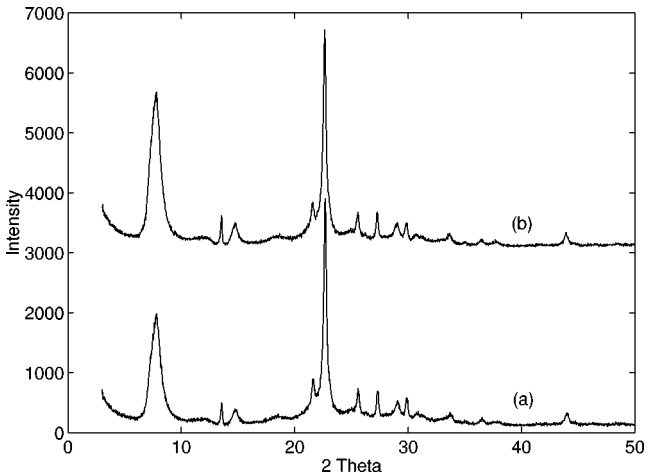

Figure 4. X-ray powder diffraction patterns of B-Beta (a) and Zr-Beta (b).

Table 1
Elemental analysis (in wt%).

	B-Beta	Zr-Beta	B-SSZ-33	Zr-SSZ-33
Boron	0.9	–	0.82	0.21
Silicon	36.5	35.88	36.78	34.81
Zirconium	–	5.32	–	2.58

Table 2
Experimental and calculated unit cell volumes (in Å^3).

	Zeolite	B	Si	Zr
Calculated	B-Beta	4196.2	4233.2	4351.2
	B-SSZ-33	3457.1	3484.4	3523.4
Experimental	Zr-Beta	4210	–	4285
	Zr-SSZ-33	3444.3	–	3456.9

The incorporation of Zr into the framework can be detected by measuring the unit cell volume of the zeolite. The unit cell volume of TS-1 has been shown to depend linearly on the amount of Ti incorporated into the framework [32,33]. Since the Zr–O bond length (1.92 Å) is much longer than the B–O bond length (1.53 Å), a substitution of B by Zr will result in an increase in the unit cell volume of the zeolite. Based on Vagard's law [2] ($V_x = V_{\mathrm{Si}} - V_{\mathrm{Si}}[1 - (d_{\mathrm{T}}/d_{\mathrm{Si}})^3]x$, where V_{Si} is the volume of the silicalite, x is the molar fraction of the T atom and d_{T} and d_{Si} are the T–O and Si–O bond lengths), one can predict the unit cell volume of a zeolite with various types of tetrahedral atom (T atom) and compare these values to experimentally measured values. The unit cell volume of the zeolite Beta and SSZ-33 are measured by indexing the X-ray powder diffraction pattern based on the polymorph A of zeolite Beta (BEA) [34–36] and the polymorph A (CON) of SSZ-33 [37,38], respectively.

For zeolite Beta, based on these calculations (table 2), we would expect a 0.9% expansion of the unit cell volume if the B of the zeolite were removed (and the Zr did not occupy a framework position). At the other extreme, for a fully incorporated Zr (in a tetrahedral coordination environment) we would expect a 3.7% increase in the unit cell volume. The experimentally determined unit cell volume increase is ∼1.8%. In the case of Zr-SSZ-33, the observed volume expansion is only 0.37% while the predicted volume expansion for the observed chemical composition is about 1.92%. These results are evidence against the complete, tetrahedral incorporation of Zr into the framework, but the treatment with $ZrCl_4$ does significantly affect the unit cell volume in the case of zeolite Beta.

If Zr is only partially grafted to the framework, then the coordination sphere of the adjacent Si atoms should be completed by OH groups (figure 5). We envision a model similar to that of vanadium in ZSM-5, which is present as V^{4+} and V^{5+} species in a distorted tetrahedral and distorted square pyramidal structure, respectively [39,40]. Silanol groups are present adjacent to the V in this zeolite.

Treatment of B-ZSM-5 with $ZrCl_4$ vapors leads to no incorporation of Zr into the zeolite. Consequently, $ZrCl_4$ can enter only through 12 MR and cannot enter through 10 MR in microporous silicates. In the case of SSZ-33, as suggested earlier, the $ZrCl_4$ enters the zeolite through the 12 MR pores alone and not through the 10 MR pores. Since the $ZrCl_4$ is only partially grafted to the zeolite framework, it prevents (or at least, slows down) the passage of other $ZrCl_4$ further into to the zeolite (figure 1). Most of the boron that is getting replaced by Zr is hence close to the crystal exterior in the 12 MR pore. Thus, the incorporation of Zr into SSZ-33 is much lower than that of Beta. For this reason, we will discuss in what follows the results from Zr-Beta only.

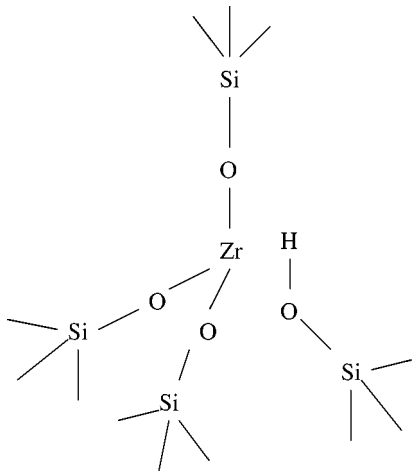

Figure 5. Zr partially grafted to the zeolite framework.

^{11}B MAS-NMR, in agreement with chemical analysis, shows that the boron content of Zr-Beta is reduced as compared to the starting B-Beta. One-pulse ^{29}Si MAS-NMR of Zr-Beta shows a Q^3 (Si connected to three other Si through oxygen, $(SiO)_3$**Si**OH) signal that is enhanced compared to B-Beta. The relative intensity of this Q^3 signal is greatly enhanced in the ^{29}Si–^{1}H CP-MAS-NMR. This observation is consistent with a partially grafted Zr atom. The protons present in the vicinity of the grafted Zr transfer their magnetization to adjacent Si, enhancing the Q^3 signal in the CP-MAS spectrum of Zr-Beta.

Consistent with the above suggestion, the micropore volume of Zr-Beta (based on the amount of N_2 adsorbed at $P/P_0 = 0.1$) was found to be 159 cm^3/g and that of B-Beta was 162 cm^3/g. The slight decrease in the micropore volume of the zeolite is consistent with Zr protruding into the zeolite pore, reducing the available micropore volume.

A comparison of the FTIR spectra of B-Beta and Zr-Beta (figure 6) shows a decrease in intensity of the peak at 1400 cm^{-1} and an enhancement in the intensity of the peak at 960 cm^{-1}. The peak at 1400 cm^{-1} has been assigned to trigonal boron [41] and a decrease in intensity of this peak is consistent with boron being removed from the framework. The 960 cm^{-1} peak has been assigned to defect silanols. An increase in intensity of this peak is consistent with defect sites generated during the reaction and as a consequence of the Zr being partially grafted to the framework.

3.1. Extra-framework Zr

We have used Raman spectroscopy to ascertain the presence of ZrO_2 clusters in our samples. The Raman spectrum of ZrO_2 shows strong characteristic peaks at 180, 390, 490 and 640 cm^{-1}. For the purpose of comparison, the Raman spectrum of a physical mixture of ZrO_2 (monoclinic) and

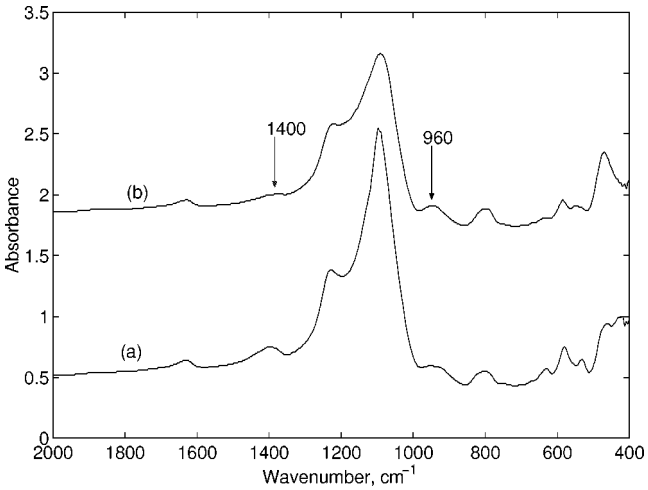

Figure 6. FTIR spectra of B-Beta (a) and Zr-Beta (b).

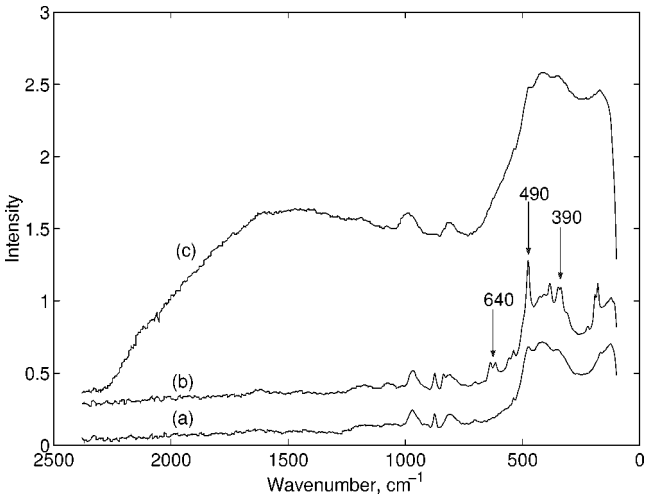

Figure 7. Raman spectra of B-Beta (a), B-Beta + 2% ZrO_2 (b) and Zr-Beta (c).

B-Beta is collected (figure 7). The Raman spectrum of the physical mixture of ZrO_2 and B-Beta shows very clearly the characteristic peaks of zirconia superimposed on the spectrum of the zeolite B-Beta. The presence of ZrO_2 in the sample can be detected in quantities much lower than 2% by weight. In contrast, though Zr-Beta shows a significant amount of fluorescence, no peaks characteristic of ZrO_2 are observed. This shows that, within the experimental resolution, there are no clusters of extra-framework ZrO_2 in our samples.

3.2. Active site characterization

The FTIR spectra of adsorbed pyridine are used to characterize the nature of acid sites in the zeolites. Hydrogen-bonded pyridine shows infrared bands at 1440–1447 cm^{-1}, 1485–1490 cm^{-1} and 1580–1600 cm^{-1}, Lewis acid sites are characterized by bands at 1447–1460 cm^{-1} and 1488–1503 cm^{-1} and Brønsted acid sites show a strong peak at 1540 cm^{-1} [42–44]. The FTIR spectrum of pyridine on B-

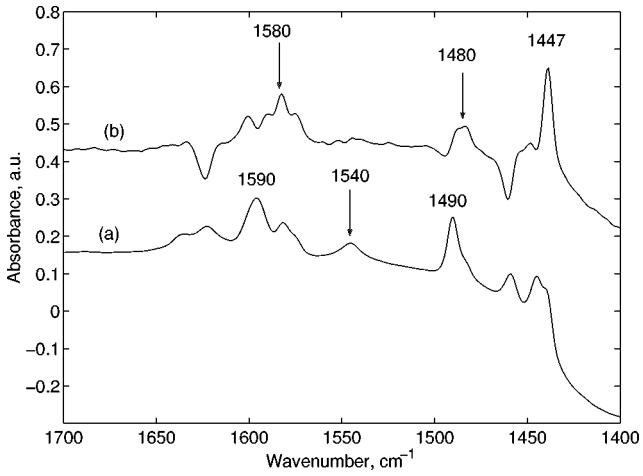

Figure 8. FTIR spectra of pyridine adsorbed on B-Beta (a) and Zr-Beta (b).

Table 3
Isopropylamine (iPA) adsorption on B-Beta and Zr-Beta.

	Mol Zr (mmol/g zeolite)	Mol iPA (mmol/g zeolite)
B-Beta	–	0.1
Zr-Beta	0.577	0.642

Beta shows peaks at 1490 and 1590 cm^{-1} (figure 8). The peak at 1450 cm^{-1} is relatively weak and disappears on raising the temperature to 100 °C. A weak peak is present at 1540 cm^{-1}. Based on these data, it can be concluded that most of the pyridine is only hydrogen bonded to the zeolite. There is no evidence for the presence of strong Lewis or Brønsted acid sites. The spectrum of pyridine on Zr-Beta is complex with an additional peak at 1447 cm^{-1}. The intensity of this peak remains strong even after evacuation at 100 °C. There is no peak at 1540 cm^{-1} and there are weak peaks at 1480 and 1580 cm^{-1}. The peak at 1447 cm^{-1} indicates the presence of Lewis acid sites and the absence of a peak at 1540 cm^{-1} indicates the absence of any strong Brønsted acid sites. The weak peaks at 1480 and 1580 cm^{-1} can be attributed to H-bonded pyridine. The $ZrCl_4$ treatment changes the character of acid sites present and most of the newly formed acid sites are Lewis sites.

We investigated the acid sites of Zr-Beta by temperature-programmed desorption (TPD) of adsorbed isopropylamine [45]. For B-ZSM-5, isopropylamine adsorbs as 1 : 1 stoichiometric complex at the B site [46]. Upon ramping the temperature, isopropylamine desorbs intact. However, in Al-containing ZSM-5, the 1 : 1 stoichiometric complex desorbs as ammonia and propylene [47]. This decomposition is due to the presence of strong Brønsted acid sites associated with the Al. The weight of the isopropylamine adsorbed on the zeolite can be used to obtain a quantitative estimation of the number of active sites present.

B-Beta adsorbs a very small amount of isopropylamine (table 3). This may be attributed to the isopropylamine physisorbed at the weak acid sites in the zeolite. Most of the

Table 4
Isomerization of 1-butene over H-Beta and Zr-Beta.

	Time on stream (min)	Conversion (%)	*Trans*/*cis* ratio	$r_A \times 10^4$ (mol/g s)
H-Beta	10	9	0.718	5.022
	50	4.3	0.687	2.4
	90	1.85	0.562	1.032
Zr-Beta	10	33.7	0.932	18.81
	50	18.4	0.918	10.27
	90	14.7	0.854	8.2

isopropylamine desorbs intact. In contrast, the mole ratio of isopropylamine to Zr is about 1 for Zr-Beta. Therefore, isopropylamine coordinates more strongly with Zr. Assuming that isopropylamine forms a 1 : 1 stoichiometric complex with Zr, then the Zr is monodispersed in the zeolite. A significant amount of isopropylamine (∼15%) desorbs as ammonia and propylene at a temperature >275 °C. The reason for this is not clear. It is likely that the desorbing isopropylamine interacts with the silanol groups present next to the Zr leading to the dissociation of isopropylamine into ammonia and propylene.

3.3. Catalysis

The conversion and activity of B-Beta and Zr-Beta for the isomerization of 1-butene to *cis*- and *trans*-2-butene is summarized in table 4. The initial activity of Zr-Beta is almost four times that of B-Beta. It might be that some of the activity of B-Beta is due to aluminum present as impurity. Our samples probably contain very small amounts of Al incorporated as an impurity (Si/Al > 500 from Ludox AS-40). However, the large difference between the activity of the Zr-Beta and B-Beta is conclusively due to the presence of Zr. Both B-Beta and Zr-Beta show significant amount of coking and consequent deactivation with time on stream. Interestingly, the deactivation rate of Zr-Beta is found to be lower than that of B-Beta. The conversion of *cis*-2-butene to *trans*-2-butene requires the presence of acid sites [49]. The *trans*/*cis* ratio obtained for Zr-Beta is higher than that obtained for B-Beta indicating that the acid sites present in Zr-Beta are more reactive than those present on B-Beta.

4. Conclusion

We have shown that upon $ZrCl_4$ treatment, Zr in Zr-Beta does not occupy a tetrahedral framework position. It is partially grafted to the zeolite framework via two or three bonds with the valence of the additional surrounding Si atoms completed by OH groups. Approximately, every atom of B is replaced by a Zr atom and the Zr is molecularly dispersed in the zeolite. We found no evidence for the presence of extra-framework clusters of Zr (in the form of ZrO_2) in Zr-Beta. The sites of the zeolite are predominantly Lewis in nature and it is found to be active in the isomerization of 1-butene to *cis*- and *trans*-2-butene.

Acknowledgement

The authors would like to thank S.I. Zones (Chevron) for providing the samples of SSZ-33. The authors would also like to thank M.E. Davis (CalTech) for obtaining the Raman spectrum and W.E. Farneth (duPont) for the isopropylamine TGA and TPD.

References

[1] G. Bellussi and M.S. Rigutto, in: *Studies in Surface Science and Catalysis*, Vol. 85, eds. J.C. Jansen, M. Stöcker, H.G. Karge and J. Weitkamp (Elsevier, Amsterdam, 1994) p. 177.
[2] G. Bellussi and V. Fattore, in: *Studies in Surface Science and Catalysis*, Vol. 69, eds. P.A. Jacobs, N.I. Jaeger, L. Kubelkova and B. Wichterlova (Elsevier, Amsterdam, 1991) p. 79.
[3] D.R.C. Huybrechts, I. Vaesen, H.-X. Li and P.A. Jacobs, Nature 345 (1987) 240.
[4] P. Ratnaswamy and R. Kumar, Catal. Today 8 (1991) 329.
[5] M. Taramasso, G. Perego and B. Notari, US Patent 4,410,501 (1983).
[6] M. Taramasso, G. Manara, V. Fattore and B. Notari, US Patent 4,666,692 (1987).
[7] C.J. Brinker and G.W. Scherer, *Sol–Gel Science* (Academic Press, Boston, 1990).
[8] R.J. Corriu and D. Leclercq, Angew. Chem. Int. Ed. Eng. 35 (1996) 1421.
[9] R.D. Shannon, Acta Crystallogr. A 32 (1976) 751.
[10] T. Takewaki, L.W. Beck and M.E. Davis, in press.
[11] J.B. Miller and E.I. Ko, J. Catal. 159 (1996) 58.
[12] S. Klein, S. Thorimbert and W.F. Maier, J. Catal. 163 (1996) 476.
[13] Z. Liu and R.J. Davis, J. Phys. Chem. 98 (1994) 1253.
[14] R.J. Davis and Z. Liu, Chem. Mater. 9 (1997) 2311.
[15] K.W. Terry, C.G. Lugmair and T.D. Tilley, J. Am. Chem. Soc. 119 (1997) 9745.
[16] R. Rulkens and T.D. Tilley, J. Am. Chem. Soc. 120 (1998) 9959.
[17] K. Tanabe, T. Sumiyoshi, K. Shibata, T. Kiyoura and J. Kitagawa, Bull. Chem. Soc. Jpn. 47 (1974) 1064.
[18] C.B. Dartt and M.E. Davis, Appl. Catal. A 143 (1996) 53.
[19] M.S. Rigutto, R. de Ruiter, J.P.M. Niederer and H. van Bekkum, in: *Studies in Surface Science and Catalysis*, Vol. 84, eds. J. Weitkamp, H.G. Karge, H. Pfeifer and W. Hölderich (Elsevier, Amsterdam, 1994) p. 2245.
[20] C.B. Dartt, C.B. Khouw, H.-X. Li and M.E. Davis, Micropor. Mater. 2 (1994) 425.
[21] T. Blasco, M.A. Camblor, A. Corma, P. Esteve, J.M. Guil, A. Martinez, J.A. Perdigon-Melon and S. Valencia, J. Phys. Chem. 102 (1998) 75.
[22] A. Zecchina, G. Spoto, S. Bordiga, A. Ferrero, G. Petrini, G. Leofanti and M. Padovan, in: *Studies in Surface Science and Catalysis*, Vol. 69, eds. P.A. Jacobs, N.I. Jaeger, L. Kubelkova and B. Wichterlova (Elsevier, Amsterdam, 1991) p. 251.
[23] A. Bittar, A. Adnot, A. Sayari and S. Kaliaguine, Res. Chem. Intermed. 18 (1992) 49.
[24] M.K. Dongare, P. Singh, P.P. Moghe and P. Ratnaswamy, Zeolites 11 (1991) 690.
[25] B. Rakshe, V. Ramaswamy and A.V. Ramaswamy, J. Catal. 163 (1996) 501.
[26] B. Rakshe, V. Ramaswamy, S.G. Hegde, R. Vetrivel and A.V. Ramaswamy, Catal. Lett. 45 (1997) 41.
[27] M.A. Camblor, A. Corma, A. Martinez, J. Perez-Pariente and S. Valencia, in: *Studies in Surface Science and Catalysis*, Vol. 82 (Elsevier, Amsterdam, 1994) p. 531.
[28] A. Corma, M.A. Camblor, P. Esteve, A. Martinez and J. Perez-Pariente, J. Catal. 145 (1994) 151.
[29] R.F. Lobo and M.E. Davis, Micropor. Mater. 3 (1994) 61.

[30] C. Fild, H. Eckert and H. Koller, Angew. Chem. Int. Ed. Eng. 37 (1998) 2505.
[31] S.I. Zones, L.T. Yuen and S.D. Toto, US Patent 5,187,132 (1993).
[32] G. Perego, G. Bellussi, C. Corno, M. Taramasso, F. Buonomo and A. Esposito, in: *Proceedings of the 7th International Conference on Zeolites*, Tokyo, 1987, p. 129.
[33] R. Millini, P.E. Massara, G. Perego and G. Bellussi, J. Catal. 137 (1992) 497.
[34] J.M. Newsam, M.M.J. Treacy, W.T. Koetsier and C.B. de Gruyler, Proc. Roy. Soc. London A 420 (1988) 375.
[35] J.B. Higgins, R.B. LaPierre, J.L. Schlenker, A.C. Rohrman, J.D. Wood, G.T. Kerr and W.J. Rohrbaugh, Zeolites 8 (1988) 446.
[36] M.M.J. Treacy and J.M. Newsam, Nature 332 (1988) 249.
[37] R.F. Lobo and M.E. Davis, J. Am. Chem. Soc. 117 (1995) 3766.
[38] R.F. Lobo, M. Pan, I. Chan, H.-X. Li, R.C. Merud, S.I. Zones, P.A. Crozier and M.A. Davis, Science 262 (1993) 1543.
[39] J. Kornatowski, B. Wichterlova, M. Rozwadowski and W.H. Baur, in: *Studies in Surface Science and Catalysis*, Vol. 84A, eds. J. Weitkamp, H.G. Karge, H. Pfeifer and W. Hölderich (Elsevier, Amsterdam, 1994) p. 117.
[40] G. Perego, R. Millini and G. Bellussi, in: *Molecular Sieves – 1; Science and Technology Synthesis*, eds. H.G. Karge and J. Weitkamp (Springer, Berlin, 1998) p. 187.
[41] D. Scarano, G. Spoto, S. Bordiga, G. Ricchiardi and A. Zecchina, J. Chem. Soc. Faraday Trans. 89 (1993) 4123.
[42] E.P. Parry, J. Catal. 2 (1963) 371.
[43] C. Paze, S. Bordiga, C. Lamberti, M. Salvalaggio, A. Zecchina and G. Bellussi, J. Phys. Chem. B 101 (1997) 4740.
[44] R. Buzzoni, S. Bordiga, G. Ricchiardi, C. Lamberti, A. Zecchina and G. Bellussi, Langmuir 12 (1996) 930.
[45] W.E. Farneth and R.J. Gorte, Chem. Rev. 95 (1995) 615.
[46] T.J.G. Kofke, R.J. Gorte and G.T. Kokotailo, J. Catal. 116 (1989) 252.
[47] D.J. Parrillo, A.T. Adamo, G.T. Kokotailo and R.J. Gorte, Appl. Catal. 67 (1990) 107.
[48] A. Ison and R.J. Gorte, J. Catal. 89 (1984) 150.
[49] A.T. Aguayo, J.M. Arandes, M. Olazar and J. Bilbao, Ind. Eng. Chem. Res. 29 (1990) 1172.